

Volume Bounds for Trivalent Planar Graphs

Anita Koh

August 2019

Abstract

The project studies the volumes of hyperbolic planar trivalent graphs. To do so we apply previous work on knots and links to graphs. In particular we use Agol-Thurston's tetrahedral upper bound and Adam's bipyramidal construction. Adam's bipyramid construction improves on Agol-Thurston. An infinite family of graphs proves this bound is asymptotically sharp.

Contents

1	Introduction	3
2	FALs and Cell Decomposition	4
3	Planar Cubic Graphs and Cell Decomposition	5
3.1	Definitions	5
3.2	Planar Graphs and FALs	6
3.3	Planar Cubic Graphs' Cell Decomposition	7
3.4	Structure of Planar Graph Embeddings	7
4	Exact Volumes	8
5	Volume Bounds	10
5.1	Lower Bound	10
5.2	Upper Bounds	11
5.2.1	Agol-Thurston's Upper Bound	11
5.2.2	Adam's Upper Bound	12
5.2.3	Putting Together Agol-Thurston and Adams	13
6	Future Research	15
7	Acknowledgements	15

1 Introduction

A *knot* is a single circular strand lying in S^3 . A *link* consists of more than one knot circle in S^3 . A *fully augmented link* (FAL) is a link whose crossings are twist reduced by removing all full twists from twist regions of the link and replacing it with a crossing disk encircling the knot circles. Each FAL can be described via perfect matchings in planar trivalent graphs. The volume of the FAL is the volume of its complement in S^3 . To see more about FALs, refer to Purcell [5]

The importance of hyperbolic geometry in topology stems from Mostow's rigidity theorem, which states that in dimension at least 3, homeomorphic objects are isometric. Thus geometric invariants become topological ones. In particular, the importance of volume in hyperbolic geometry is that each hyperbolic knot and link is associated with a unique volume which can be used as an invariant to identify properties of that knot or link.

There are many different upper bounds on volume in hyperbolic geometry for different types of hyperbolic links. One previous result by Agol and Thurston in an appendix to Lackenby [3] is the upper bound for hyperbolic links,

$$Vol(S^3 - L) \leq 10v_3(t(D) - 1),$$

where $t(D)$ is the number of twist regions.

A result by Adams [1] uses bipyramids to bound the volume of hyperbolic alternating links. He proves the bound

$$Vol(S^3 - L) \leq \sum b_i Vol(B_i) - a.$$

For constants, read further. Adams shows that this upper bound improves upon that of Agol-Thurston because bipyramids have less volume than the corresponding tetrahedral decomposition.

One natural generalization of links is embedded graphs in S^3 . The overarching focus of this paper is to use Adams bipyramid construction to bound volumes of planar cubic graphs that are hyperbolic. Heard, Hodgson, Martelli and Petronio initiated a study of trivalent graphs embedded in 3-manifolds, classifying the simplest ones [3].

Masai made a connection between planar cubic graphs in S^3 and FALs, and considered upper bounds for volumes of such graphs [5]. Here we extend Masai's investigation by combining his results with Agol-Thurston, Adams and Purcell. More precisely we find:

1. exact volume bounds for graphs with at most 12 vertices,
2. sharp lower bounds for graphs with n vertices,
3. upper bounds for hyperbolic graphs,
4. examples of cubic planar graphs whose upper bound is asymptotically sharp.

2 FALs and Cell Decomposition

Before discussing FALs or fully augmented links, some definitions are needed. *Full twists* is when two link strands cross over one another twice.



Figure 1: Left: 1 full twist. Right: 3 full twists

When a link is *twist reduced* all twists for a collection of knot strands are grouped in a single region. That region is called the *twist region*, a tangle in the diagram where two knot strands twist.



Figure 2: Left: twist reduced link. Right: not twist reduced link.

A *fully augmented link* (FAL) is a twist reduced link where a trivial component is placed around each twist region and full twists are removed. Each FAL can be described via perfect matchings in planar trivalent graphs. See Purcell [4] for more about FALs.

To see the hyperbolic structure we describe a cell decomposition of $S^3 - L$. The components of the cell decomposed FAL are

- 0-cells: None, otherwise they would be the endpoints of the edges which correspond to ideal points.
- 1-cells: Intersections of planar and crossing disks.
- 2-cells: The crossing disks, and planar cells.
- 3-cells: Everything above and below the projection plane, \mathbf{B}_+^3 and \mathbf{B}_-^3 .

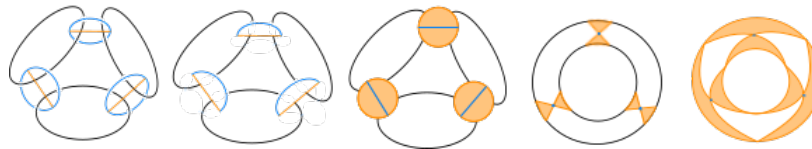


Figure 3: Polyhedral decomposition of an FAL

To obtain the polyhedral decomposition of an FAL:

1. Slice along planar two cells or knot circles. Since P_+ and P_- are reflections of one another across the projection plane, lets focus on P_+
2. Slice crossing disks along the 1 cells and flatten out.
3. Shrink crossing arcs, so now the crossing disks look like bow ties.
4. Shrink knot circles.

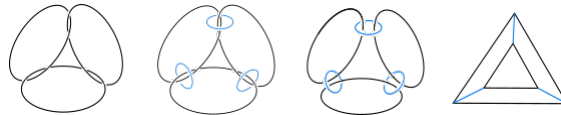


Figure 4: Example of turning link into FAL and its corresponding graph

Ideal points on the cell decomposition of an FAL are the points where two of the unshaded regions and two of the shaded regions meet, the corners of the triangles of the bow ties.

Remark: to get from P_+ and P_- to the FAL, glue P_+ and P_- .

A *circle packing* is the cell decomposition's regions and how those regions are adjacent represented in a diagram. A circle packing converts unshaded regions to circles and the circles' tangent edges respectively.

There are two combinatorial ways to describe this polyhedral decomposition. The first way is the *nerve* which is a graph composed of triangular faces. Each vertex representing the center of circles in the circle packing and all edges represents the points of tangency between the circles in the circle packing. Another way to represent the polyhedral decomposition is the *dual*. The *dual* of a planar graph is when a vertex is set on each face of the original graph and connected by edges going through the original graph's edges. Here the polyhedral decomposition can be represented as the dual of the nerve, where every vertex represents a face in the nerve and each edge the tangency between the faces in the nerve.

3 Planar Cubic Graphs and Cell Decomposition

3.1 Definitions

The words *trivalent*, *cubic*, and *3-regular* will be used synonymously to describe graphs where each vertex has degree 3.

A *perfect matching* in a graph is a pairing of adjacent vertices.

Perfect matchings in trivalent graphs are clearly seen in the *well-painted* graphs of Purcell where the edge between paired vertices is colored, each vertex only having one colored edge. Purcell shows that perfect matchings correspond to FALs.

The *medial graph* G_m of a graph G , is defined to have midpoints of edges of G as vertices, with edges connecting nearby midpoints.



Figure 5: Example of perfect matchings on the 6 vertex graph

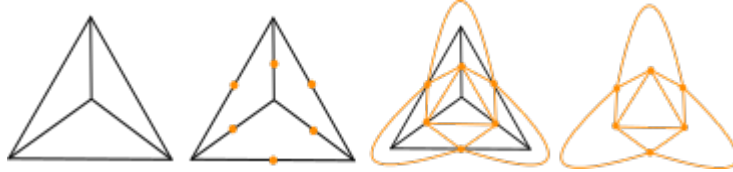


Figure 6: Process of creating a medial graph from a dual: placing vertices on midpoints of edges, connecting vertices based on the adjacency of dual's faces, the medial graph.

The medial graph G_m of a planar cubic graph G cuts the plane into regions that can be checkerboard colored so that each shaded face is triangular. The shaded triangles contain the vertices of the original graph G .

There is a connection between the checkerboard coloring of G_m circle packings of FALs. More precisely the shaded triangles of G_m are the shaded portions of the circle packing.



Figure 7: Dual, dual's medial graph, and circle packing

3.2 Planar Graphs and FALs

Note that shrinking the edges of a dual within the medial graph results in cell decomposition of the dual, which in turn corresponds to the FAL. With a medial graph, each shaded triangle corresponds of the shaded regions or bow ties that appear in an FAL's cell decomposition. Thus the FAL complement corresponds to a perfect matching on a planar trivalent graph G , and the manifold $S^3 \setminus G$ are made from the same polyhedra P_+ and P_- . The only difference between $S^3 \setminus G$ and the FAL is that shaded triangles are not glued to form $S^3 \setminus G$.

The different matchings of a planar trivalent graph correspond to FALs of different polyhedral gluings, but both correspond to the same circle packing.

This correspondence between FALs and planar trivalent graphs implies that

their respective volume bounds also correspond.

3.3 Planar Cubic Graphs' Cell Decomposition

We have already seen that planar trivalent graphs arise naturally in the FAL setting. In fact, authors have studied them directly

Letting M be a closed, connected, orientable 3-manifold and G denote some trivalent planar graph; when the meridian of edges of a graph correspond to parabolic isometries then $M \setminus G$ is a hyperbolic manifold with the boundary as the thrice punctured spheres. This boundary on the graph is located at each vertex. This boundary represents a thrice punctured sphere when one envisions a sphere encircling a vertex and the edges radiating from the vertex of the trivalent graph creating three punctures in the sphere. Refer to Heard, Hodgson, Martelli and Petronio [3] for more information regarding parabolic isometries.

Remark: to get from P_+ and P_- to the graph, only glue the unshaded faces together

The resulting components of the cell decomposition of a cubic planar graph are

- 0-cells: None, since ideal polyhedrons are used
- 1-cells: Intersection of the spheres with the projection plane
- 2-cells: The thrice punctured spheres and the projection plane
- 3-cells: The regions above and below the plane, B_+ and B_-

To obtain a cell decomposition of a planar cubic graph, referring to figure:

1. Replace each vertex with a sphere. Each edge makes a puncture on the sphere.
2. Shrink graph edges to obtain P_+ and P_-



Figure 8: Cell decomposition of the planar graph

3.4 Structure of Planar Graph Embeddings

Planar graphs have associated equations which can be utilized in finding the volume. One such equation is the Euler characteristic, letting V be the number of vertices, E edges and F faces, we have

$$V - E + F = 2.$$

Given the paper's sole use of trivalent graphs, another applicable equation is

$$3V = 2E.$$

Trivalent graphs have this property because each vertex is degree three, or has three edges coming out of each vertex. Since each edge has a vertex on either end, every edge is counted twice when summing all edges coming out of each vertex.

4 Exact Volumes

Now that we have an explicit constructing for the hyperbolic structure on the complement of planar trivalent graphs in S^3 , let's proceed with explicit volume calculations for graphs with fewer vertices. Initially we determined which trivalent graphs in the table simple cubic graphs [7] are planar. To find the volume of planar ones, we used perfect matchings to find associated FALs, then used the *SnapPy* program to compute the volume. The limitation to this method was that after 12 vertices, there would be too many graphs to find the volumes by hand, as well as *SnapPy*'s inability to take in more than a certain number of components when drawing the FAL into the program. The volumes of the maximum volume graph of a certain number of vertices is compared with Agol-Thurston's bound and Adams's collapsed bipyramidal construction below. This coincides with and extends Masai's calculations in [5].

Vertices	Maximum Volume	Agol-Thurston	Adams
4	7.3277	10.1494	8.1192
6	14.6554	20.2988	15.8426
8	24.0922	30.4482	24.1882
10	32.5515	40.5676	35.8803
12	41.4162	50.747	45.8095

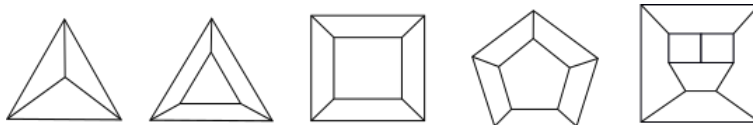


Figure 9: The maximum volume graphs in ascending vertex count order.

For the 4 and 6 vertex graphs, there is only one possible trivalent planar graph, so those graphs are also their respective vertex count's minimum volume graph.

Multiple things were tried in order to find a pattern between the maximum volume graphs and to see how they differed from the graphs of the same number

of vertices but lower volumes. For vertex count 4 to 10, it seemed that nested $\frac{V}{2}$ -gons were the maximum volume graphs, but the 12 vertex maximum graph refuted that possibility.

Then I compared the FALs of the graphs with 4 to 12 vertices and observed that the higher volume graphs had fewer belt-sum decompositions. In comparing the graphs, the graphs with the same volume were non-prime graphs. This is because the 3-cuts in those graphs corresponds to the thrice punctured sphere. Slicing through those 3-cuts topologically corresponds to summing the volumes of both graphs on either side of the slicing. See Adams [2].

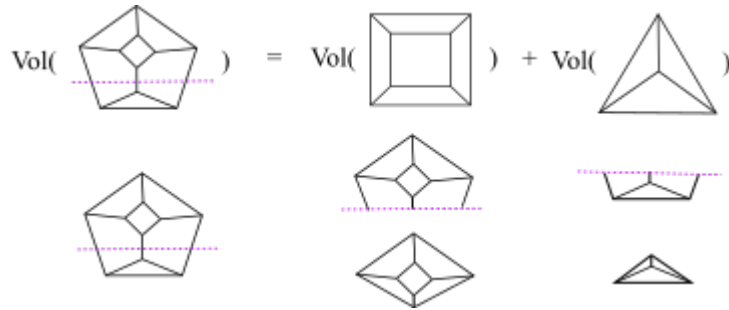


Figure 10: Slicing and 10 vertex graph along a 3-cut. Cut edges are joined at a new vertex. So the volume of the 10 vertex graph is the sum of the 2 prime graphs.

Each maximum volume graph was a prime graph for its number of vertices. It was also observed that each maximum volume graph had the highest n-cut for its number of vertices, so that allowed me to ignore the 3-cut 12 vertex trivalent planar graphs in analyzing graphs for the maximum volume.

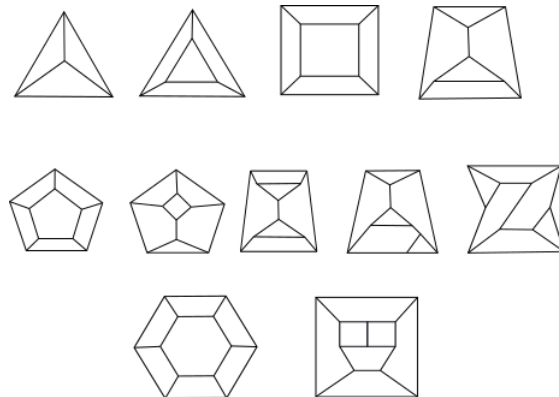


Figure 11: The following table's graphs from left to right going down: 4, 6, 8.1, 8.2, 10.1, 10.2, 10.3, 10.4, 10.5, 12.1, 12.2.

Graph	3-edged face	4	5	6	Volume	Uncollapsed Bipyr Vol
4	4	0	0	0	7.3276	16.2384
6	2	3	0	0	14.6552	27.2298
8.1	0	6	0	0	24.0921	38.2212
8.2	2	2	2	0	21.98	37.599
10.1	0	5	2	0	32.5515	48.5904
10.2	1	3	3	0	31.4199	48.2793
10.3	2	3	0	2	29.3109	47.5282
10.4	3	0	3	1	29.3109	47.4371
10.5	2	2	2	1	29.3109	47.7482
12.1	0	6	0	2	41.4162	58.5196
12.2	0	4	4	0	40.5977	58.9596

From there I read more about Agol-Thurston's upper bound and Adam's improvement upon it. I calculated the bipyramidal volume for each graph (without collapsing) by hand after calculating the number of faces and edges bounding however many faces by hand. Seeing that Adams gave the best upper bound, I tried extending it by using the number of vertices a graph had to determine sizes of the graphs faces, but reached a dead end. Attempting to generalize the bound to use the number of vertices to determine the sizes of the faces had issues in fitting into the numerical requirements of a linear equation, but not meeting the Euler characteristic or trivalent property. There was no pattern in the number of faces or the size of faces correlating with which graph had the maximum volume.

5 Volume Bounds

5.1 Lower Bound

A lower bound for volumes of hyperbolic FALs appears in [5], whose Proposition 3.6 states

Proposition [Purcell]: If L is a hyperbolic fully augmented link with c crossing circles, then

$$\text{vol}(S^3 - L) \geq 2v_8(c - 1)$$

where $v_8 = 3.66386\dots$ is the volume of a regular ideal octahedron. Moreover

$$\text{vol}(S^3 - L) = 2v_8(c - 1)$$

if and only if $S^3 - L$ decomposes into regular ideal octahedra.

Thus this bound is sharp. Refer to figure 10 for the following explanation. Purcell observes that each successive central subdivision of a triangle within the nerve adds a circle in one of the triangle's in the nerve's circle packing. The adding of a circle in a triangle of the circle packing is the same as adding an ideal regular octahedron. The central subdivision of a nerve is equivalent to turning a vertex of the trivalent graph into three vertices. In taking a dual

of a graph, each former vertex is surrounded by tangencies of the faces across previous edges. The trivalent graph's original vertex is a triangular face in the nerve. By turning the trivalent graph's vertex into three vertices, we are equivalently centrally subdividing the triangular face that vertex is. Since both are equivalent, Purcell's lower bound for volume is sharp for trivalent graphs and their corresponding hyperbolic link.

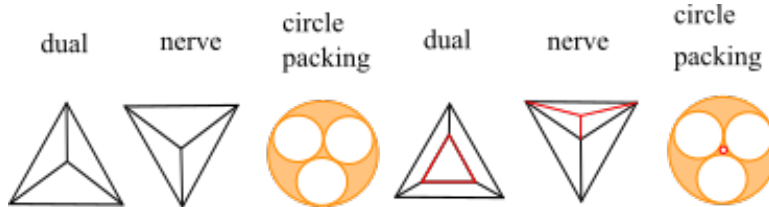


Figure 12: Left to right: Example of 4 vertex graph with its nerve and circle packing then the 6 vertex graph as added vertices and central subdivision in its nerve with the added circle in its circle packing

5.2 Upper Bounds

This paper will apply techniques of upper bounds for different kinds of hyperbolic links to the trivalent graph setting. In particular, we will draw from Adam's bipyramidal construction and apply them to planar trivalent graphs and Agol-Thurston's bound utilizing tetrahedra.

5.2.1 Agol-Thurston's Upper Bound

Agol-Thurston improved Lackenby's [3] upper bound for the volume of links K with a prime alternating diagram D . Their upper bound was

Theorem[Agol-Thurston]: Given a projection diagram D of a link L with twist number $t(D)$ then

$$\text{vol}(S^3 - L) \leq 10v_3(t(D) - 1)$$

Moreover there is a sequence of links L_i such that

$$\text{vol}(S^3 - L)/t(D_i) \rightarrow 10v_3$$

Overview of Agol-Thurston's Proof: Agol-Thurston prove their theorem by first creating an augmented alternating link L then cellularly decomposing L . Tetrahedra are then placed on each shaded link region, one on P_+ and one on P_- . Noting that each twist region decomposes into 2 shaded regions, the bow tie, there are $4t(D)$ tetrahedra on the shaded regions. The unshaded regions are divided into as many tetrahedra as there are sides of the unshaded region. Also noting that each twist region is tangent to 2 unshaded faces, and that the unshaded faces must be at least 3-sided, then the number of tetrahedra given

by the unshaded faces is at least $6t(D)$. Hence, the total number of tetrahedra so far is $10t(D)$. Afterwards, Agol-Thurston collapse tetrahedra. To collapse tetrahedra, choose an ideal vertex. Since every 2 unshaded regions have at least 6 tetrahedra and every 2 shaded regions have 4, we may collapse 10 tetrahedra, resulting in

$$\text{vol}(S^3 - L) \leq 10v_3(t(D) - 1).$$

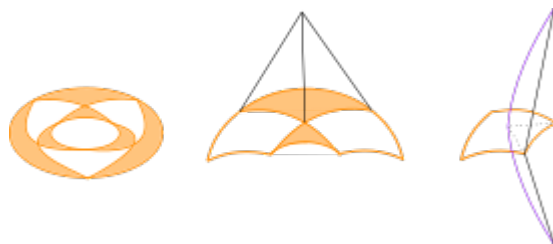


Figure 13: Placement of tetrahedra on shaded regions and stellar subdivision of unshaded regions into tetrahedra.

For more detail, please view Agol-Thurston's proof in full in their appendix to Lackenby [3].

5.2.2 Adam's Upper Bound

Adams improved on the Agol-Thurston upper bound for hyperbolic alternating links using a bipyramidal construction. By using bipyramids through the faces of the augmented link instead of stellar subdivisions and placing tetrahedra on all faces the process is much more efficient. An additional benefit to Adam's bipyramid construction is the fact that the volume of an n -sided bipyramid is always less than the volume of the sum of n tetrahedra. Refer to Adams [1] for more detail on his upper bound for hyperbolic alternating links.

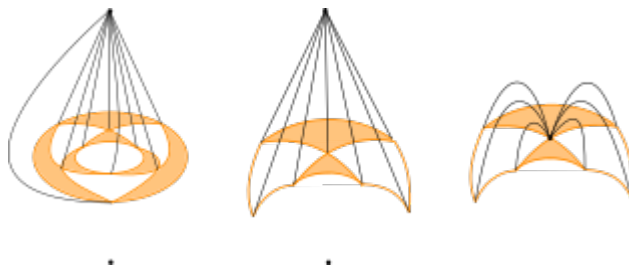


Figure 14: The upper half of bipyramids on an FAL and the local collapsing at a chosen ideal point

In figure 11, the upper half of bipyramids is displayed on the polyhedral cell decomposition. The top point of the bipyramids goes to the vertices above

and below the projection plane, one placed in P_+ and one in P_- . The first image displays only the top half of the bipyramids for clarity. The second image displays the regions around a chosen ideal point. The third displays the flattening of the upper half of the bipyramids when shrinking the edge at the ideal point. This collapsing at the ideal point also happens in the lower half.

5.2.3 Putting Together Agol-Thurston and Adams

Agol-Thurston show their upper bound is asymptotically sharp by doing complex polyhedral gluings on the infinite chain link fence. Taking our cue from their work, we show the bipyramid upper bound is asymptotically sharp for trivalent planar graphs. We have prove then

Theorem: Given a planar trivalent graph having V vertices and bipyramidal upper bound (BUB)

$$BUB \leq 10v_3(\frac{V}{2} - 1)$$

And there is a sequence of graphs G where

$$BUB/\frac{V}{2} \rightarrow 10v_3$$

Proof. : To obtain this upper bound we break down Agol-Thurston's chain-link fence by beginning with smaller graph constructions of the chain link fence (see Figure 13).

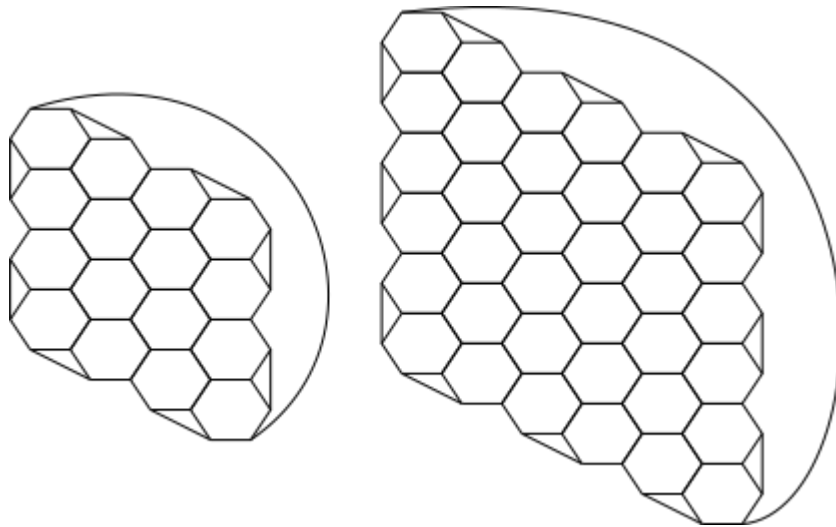


Figure 15: Smaller graph constructions of the infinite chain-link fence, H_4 and H_6 .

The graph H_m cuts the plane into polygonal faces. We begin by counting the number of faces of each type. It can be noted that there are m^2 hexagonal faces,

$m = 4, 6, 8, \dots$. There are also $2m$ triangular faces. The two $2m$ -sided faces are the largest faces. Recall Adam's bipyramidal construction in section 5.2.2. We will be collapsing the 2 largest faces since their sharing of an edge in the planar trivalent graph translates to an ideal point in the FAL's cell decomposition. We also need the number of vertices, which will each have a 3-sided bipyramid through them when computing the volume, except for the 2 collapsed at the ideal point. To obtain this number, we shall utilize the Euler characteristic and the graph's trivalent property. Recall that we know $F = m^2 + 2m + 2$, $3V = 2E$ and $V - E + F = 2$. Substituting, we have

$$\begin{aligned} V - E + F &= 2 \\ V - \frac{3V}{2} + m^2 + 2m + 2 &= 2 \\ m^2 + 2m &= \frac{V}{2} \\ 2m^2 + 4m &= V. \end{aligned}$$

Using Adams bipyramidal construction we place n -sided bipyramids on all n -sided faces and 3-sided bipyramids on all vertices. Finally we collapse the two largest faces together with the adjacent shaded triangles. We then see

$$\begin{aligned} BUB &= m^2 \text{vol}(B_6) + (2m + 2m^2 + 4m - 2) \text{vol}(B_3) \\ &= m^2 \text{vol}(B_6) + (2m^2 + 6m - 2) \text{vol}(B_3). \end{aligned}$$

Noting $\text{vol}(B_6) = 6v_3$ and $\text{vol}(B_3) = 2v_3$ (see Adams[1]), upon dividing both sides by half the number of vertices and taking a limit as m goes to infinity

$$\begin{aligned} \lim_{m \rightarrow \infty} \frac{BUB}{m^2 + 2m} &= \lim_{m \rightarrow \infty} \frac{m^2 6v_3 + (2m^2 + 6m - 2)2v_3}{m^2 + 2m} \\ &= \lim_{m \rightarrow \infty} \frac{m^2 6v_3 + m^2 4v_3 + m 12v_3 - 4v_3}{m^2 + 2m} \\ &= \lim_{m \rightarrow \infty} \frac{m^2 10v_3 + m 12v_3 - 4v_3}{m^2 + 2m} \\ &= 10v_3, \end{aligned}$$

Since Adam's shows that his bipyramid construction is always at most the tetrahedral constant of Agol-Thurston, we have

$$BUB < 10v_3 \left(\frac{V}{2} - 1 \right)$$

□

Despite supporting that $10v_3$ is an optimal coefficient to the upper bound on volume, there are still several unknowns in the bipyramidal volume construction for trivalent graphs. Since this paper works with small trivalent graphs, the hexagonal construction may not be the graph of the maximum volume for however many vertices it has.

6 Future Research

Many roadblocks in this project can be explored more extensively to find potentially lovely results.

- Is there any way to further improve the bipyramid bound?
- What would be done for links represented by non-planar graphs?
- Show that non-prime graphs also reach the upper bound for large enough n vertices
- Is there a lower bound for the hexagon family graphs?
- Can Lackenby's article on guts of surfaces be used to find a lower bound on the maximum volume of graphs?
- Is there a way to prove that prime and highest connected graph for the number of vertices a graph has are the graphs with maximum volume?

7 Acknowledgements

I would like to thank Rolland Trapp for guiding this research, the whole CSUSB 2019 REU group, CSUSB for hosting the summer research and the NSF for funding this research with grant 1758020.

References

- [1] C. Adams, 'Bipyramids and bounds on volumes of hyperbolic links', *Topology Appl.* 222 (2017) 100–114.
- [2] C. Adams, Thrice-Punctured Spheres in Hyperbolic 3-Manifolds, *Transactions of the American Mathematical Society* 287, no. 2, pp. 645–656 (1985).
- [3] D. Heard, C. Hodgson, B. Martelli, C. Petronio, Hyperbolic graphs of small complexity, *Experiment. Math.* 19 (2010), 211-236.
- [4] M. Lackenby, *The Volume of Hyperbolic Alternating Link Complements*, 1-30.
- [5] H. Masai, *On Volume Preserving Moves on Graphs with Parabolic Meridians*, 88-93.

- [6] J.S. Purcell, *An introduction to fully augmented links*, *Interactions between hyperbolic geometry, quantum topology and number theory*, Contemp. Math. 541 Amer. Math. Soc., Providence, RI, (2011) 205-220.
- [7] Wikipedia contributors. "Table of simple cubic graphs." Wikipedia, The Free Encyclopedia. Wikipedia, The Free Encyclopedia, 14 Aug. 2019. Web. 14 Aug. 2019.
- [8] W.P. Thurston, *The geometry and topology of three-manifolds*, Princeton Univ. Math. Dept. Notes, 1979.